Machine learning algorithms for predicting scapular kinematics

Kristen F. Nicholson [a,*], R. Tyler Richardson [b], Elizabeth A. Rapp van Roden [a],
R. Garry Quinton [a], Kert F. Anzilotti [c], James G. Richards [a]

[a] *Biomechanics and Movement Science Program, University of Delaware, Newark, DE, USA*
[b] *Kinesiology Program, School of Behavioral Sciences and Education, Penn State Harrisburg, Middletown, PA, USA*
[c] *Department of Radiology, Christiana Health Care System, Newark, DE, USA*

ARTICLE INFO

ABSTRACT

The goal of this study was to develop and validate a non-invasive approach to estimate scapular kinematics in individual patients. We hypothesized that machine learning algorithms could be developed using motion capture data to accurately estimate dynamic scapula orientation based on measured humeral orientations and acromion process positions. The accuracy of the algorithms was evaluated against a gold standard of biplane fluoroscopy using a 2D to 3D fluoroscopy/model matching process. Individualized neural networks were developed for nine healthy adult shoulders. These models were used to predict scapulothoracic kinematics, and the predicted kinematics were compared to kinematics obtained using biplane fluoroscopy to determine the accuracy of the machine learning algorithms. Results showed correlations between predicted kinematics and validation kinematics. Estimated kinematics were within 10 of validation kinematics. We concluded that individualized machine learning algorithms show promise for providing accurate, non-invasive measurements of scapulothoracic kinematics.

© 2019 IPEM. Published by Elsevier Ltd. All rights reserved.

1. Introduction

The shoulder is a complex system consisting of multiple joints: glenohumeral, sternoclavicular, acromioclavicular, and scapulothoracic (ST). To better understand and treat shoulder pathologies, precise measurement of the entire shoulder joint complex is required. However, precise measurements of ST kinematics are challenging to obtain. The relatively independent movement between the scapula and the skin surface complicates the measurement of scapular motion. Previous studies on shoulder kinematics commonly describe the orientation of the humerus relative to the thorax, neglecting the important role of the scapula as an intermediary structure [1]. Abnormal scapular movement is an important factor in the clinical pathology of the shoulder joint, and there is significant need to obtain clinical measures of scapular kinematics [2–5]. Improved understanding of scapular kinematics and shoulder motion during dynamic activities in healthy and pathologic joints will inform treatment and rehabilitation of shoulder injuries and pathologies [6].

Despite the need for accurate scapular kinematics, a measurement technique that can be used in the clinical setting on all patients and all motions has yet to be developed. Current techniques used to measure scapula orientation are either inaccurate for particular populations, invasive, time consuming, limited to static positions, require expensive equipment, or have not been validated for all motions, decreasing their clinical utility [7–13].

Scapula motion is governed by two constraints: the attachment to the clavicle, and the contact surface formed by the rib cage. Because the surface of the rib cage is non-planar, the scapula can change orientation indirectly through displacements such as elevation, or directly by actions of the muscles that anchor the scapula to the trunk. Since the primary function of the scapula is to serve as the base of support for the humerus, scapula orientation is related to the orientation of the humerus. Thus, knowledge of the position of a measurable displacement landmark such as the acromion process (AP), combined with measures of the orientation of the humerus, may be adequate to estimate the actual orientation of the scapula. The contact surface between the scapula and the rib cage can vary between individuals, and these variations may be exaggerated in pathologies. Furthermore, these pathologies can have profoundly diverse effects on the function of the glenohumeral joint. As a result, prior statistical approaches to estimating scapula orientation based on group measures have little value when examining an individual patient. In this study, traditional motion capture was utilized to develop individualized

---

Abbreviations: ST, scapulothoracic; TS, trigonum spinae; IA, inferior angle; AP, acromion process.

* Corresponding author.

E-mail addresses: kristent@udel.edu (K.F. Nicholson), tr12@psu.edu (R.T. Richardson), lizrapp@udel.edu (E.A.R. van Roden), drrgquinton@gmail.com (R.G. Quinton), kanzilotti@christianacare.org (K.F. Anzilotti), jimr@udel.edu (J.G. Richards).

Fig. 1. Experimental setup. Subjects lie prone inside the viewing volume of the fluoroscope and the motion capture cameras.

machine learning algorithms to estimate each individual's scapular kinematics. The approach described in this paper utilized static measures of scapular displacement and humeral orientation to develop algorithms that provide reliable and accurate measures of scapula orientation in all positions for that individual. It was expected that these algorithms could be applied to dynamic motion capture measures to provide an estimate of scapular motion.

2. Materials and methods

Since the development of individualized algorithms and identification of within subject differences were the primary focus, nine subjects constituted a sufficient population to develop the machine learning algorithms and to demonstrate the applicability of the algorithm across an array subjects. All subjects were free of shoulder pain and dysfunction, and had no history of shoulder injury or surgery.

Bone pins have previously been used as the gold standard for determining dynamic scapula orientation [1,14,15]. However, there is reason to believe that scapula movement is constrained when pinned to the skin [16]. Therefore, a biplane fluoroscopy image matching technique was utilized as the standard for validation [17].

Each subject lay prone on a bench inside the view of a clinical fluoroscope [18] and seven motion capture cameras (Motion Analysis Corporation, Santa Rosa, CA) (Fig. 1). 3D retroreflective markers 6 mm in size were placed on the trunk, scapula, and arm: three markers on a thin rigid plank adhered to the spine, AP, trigonum spinae (TS), inferior angle (IA), lateral and medial epicondyles of the elbow. The center spine marker was placed on a post to avoid collinearity. The markers were used to create trunk, humerus, and scapula coordinate systems in accordance with International Society of Biomechanics recommendations [19]. Three-dimensional coordinate data were recorded at 60 Hz. Biplane fluoroscopy (BV Pulsera, Philips Medical Systems, USA) images were recorded with two C-arms: one capturing images in the sagittal plane, the other capturing images 103° from the first C-arm. The fluoroscopy data were recorded at 12.5 pulses/s.

Each subject completed two dynamic motion trials while simultaneously undergoing biplane fluoroscopy and 3D motion capture. Prior to starting each motion trial, the position of the C-arms was adjusted to optimize the viewing volume and ensure the scapula remained in the view throughout the motion. The dynamic motion trials encompassed a total of eleven positions: a neutral position, six modified Mallet positions [20], and four additional positions of maximal humeral elevation, humeral extension, humeral flexion, and forward reach, as if grasping for an object on the floor (Fig. 2). These positions were chosen as they exemplify acts of daily living and include the entire range of humeral and scapula motion. The first dynamic motion trial consisted of starting in the neutral position, then continuously moving through abduction, hand to mouth, hand to neck, and elevation. The second dynamic motion trial consisted of starting in the neutral position, then continuously moving through forward reach, extension, hand on spine, external rotation, internal rotation, and flexion. A metronome, at 60 bps, was played to assist the subject in timing. They were instructed to achieve each position in two metronome beats. If the subject conformed to this pace, the first trial lasted 8 s, and the second trial lasted 12 s. The total fluoroscopy time was monitored to ensure the subject did not receive more than 30 s of radiation exposure. Subjects were allowed several practice trials with no data collection. A certified radiology technician operated the fluoroscopy for each subject.

After the motion trials, one second of three-dimensional motion capture data was collected while the subject held each of the eleven positions. Subjects were instructed to strive for maximum excursion in all static positions. Once maximum excursion was achieved, the TS and IA were palpated and marked with 3D retroreflective markers. The subject held the position while 3D motion capture data were collected.

Custom software was used to align the trunk and a scaled 3D model to the fluoroscopy images following the technique described by Nicholson, et al. [17]. The angle between the matched trunk and the matched scapula was calculated and used to determine the 3D orientation of the scapula in the trunk's coordinate system (Fig. 3). The scapula kinematics determined from these trials were used as
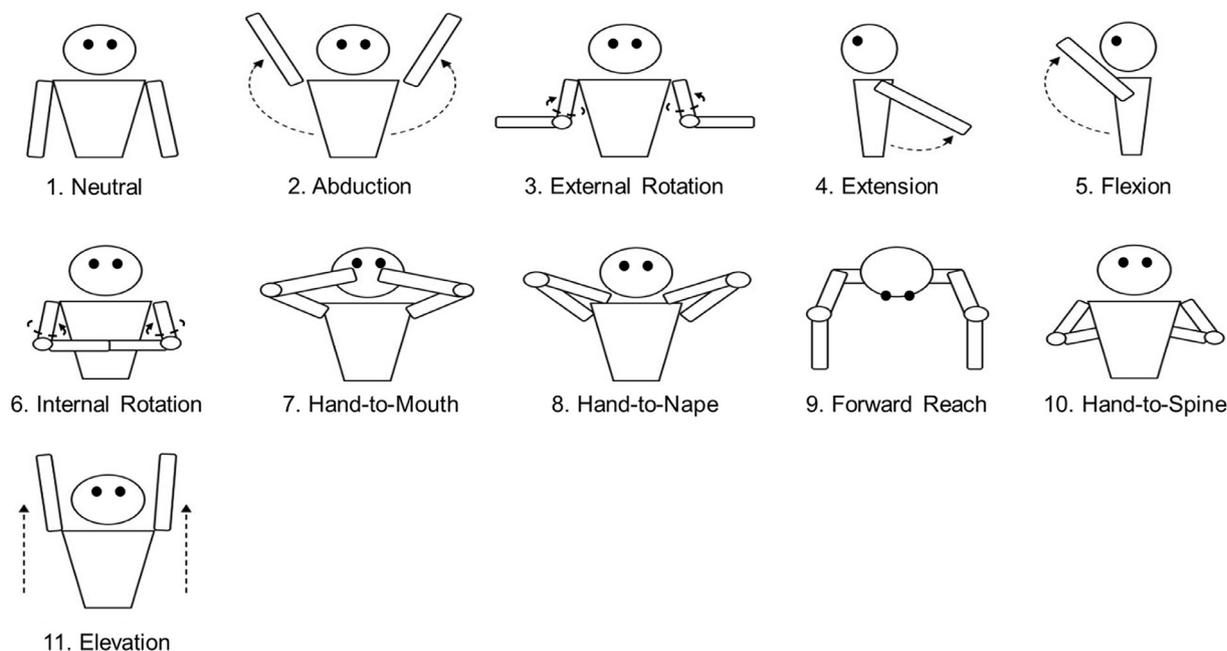
Fig. 2. The motion trials encompassed eleven positions. A neutral position, the six Modified Mallet positions, elevation, extension, flexion, and forward reaching.

the standard for validating the machine learning algorithms created from the motion capture data.

Algorithm development is based on the principle that scapula orientation is a function of humeral orientation and acromion process displacement. For any given humeral orientation and AP displacement, the scapula orientation is expected to be consistent, regardless of the path of motion used to reach that position. Mathematical algorithms were created for each subject using data from the eleven static positions. All 60 frames of data for each of the static positions were used, creating a 660 point input data set. Humeral orientation and AP displacement were algorithm inputs. Humeral orientation was calculated as humerothoracic helical angles, i.e. the helical angle between the trunk and the humerus, and AP displacement was calculated as the displacement of the AP marker along the Y axis (inferior/superior) and the X axis (anterior/posterior). Since the AP is attached to the clavicle, the displacement along the Z axis was expected to be negligible, and was not used as an input to the algorithm development. The predicted values were scapula orientation, calculated as the X, Y and Z components of the ST helical angles, i.e. the helical angle between the trunk and the scapula. Algorithms were developed using artificial neural networks.

Artificial neural networks are statistical machine learning algorithms inspired by biological neural networks in the brain. They are currently used as a tool for analysis, prediction, control, identification, and/or data processing. The artificial neural network consists of neurons grouped in neuron layers. A typical network has an input neuron layer, a hidden neuron layer, and an output neuron layer. Artificial neural networks have an adaptive nature making them capable of learning and pattern recognition. A resulting network can compute values from inputs, similar to multiple linear regression algorithm, however the relationship between inputs and outputs does not have to be linear. Artificial neural networks can be distinguished by type, structure, and learning algorithm. For this study, a feed-forward, back-propagation artificial neural network program (aNETka version 2.0, created by Stan Zurek, Wolfson Centre for Magnetics, Cardiff University, Cardiff, United Kingdom) was used to create predictive networks for each individual's ST X component, ST Y component, and ST Z component. Each neuron in the hidden layer(s) collects the input values multiplied by

a weight matrix and processes them with an activation function (Fig. 4).

Algorithms derived from neural networks were applied to AP displacement and humerus orientation measures obtained from the motion capture data collected during the dynamic trials. The resulting ST angles were interpolated to 300 frames per second using a linear interpolation algorithm. Every 24th angle was extracted so the algorithm determined ST angles aligned with the 12.5 frames per second collected by the fluoroscope. Every 4th angle of the resulting subset was then compared to the angles obtained from matching the 3D models to every 4th fluoroscopy frames. By comparing the estimates of scapula orientation derived from the algorithms to the corresponding scapula orientations measured using the validation standard, a direct assessment of the error associated with the estimates could be made.

Accuracy of each neural network was determined through correlations and absolute mean differences. The strength of the correlations were assessed according to Evans (0.00–0.19: very weak, 0.20–0.39: weak, 0.40–0.59: moderate, 0.60–0.79: strong, 0.80–1.0: very strong) [21]. An algorithm was deemed clinically accurate if the absolute mean difference between the algorithm's estimated ST angles and the fluoroscopy determined ST angles was less than ten degrees around each axis.

3. Results

Several configurations of a feed-forward back-propagation neural network were explored. User defined options include the number of layers, the number of neurons per layer, the activation function (linear, sigmoid/logistic, or hyperbolic tangent), the learning rate, the maximum number of iterations, the stopping criterion (an acceptable RMSE), and the number of training vs. test points. The network configuration that performed the best had one hidden layer with eleven neurons, used a sigmoid/logistic activation function, and had a learning rate of 0.1. The input data for each network was divided into training cases and test cases, with 90% of the data points serving as training cases and 10% as test cases. A network's training was completed when one of three conditions was met: the maximum number of iterations had been completed (10,000), the stopping criterion had been met (RMSE of 1),
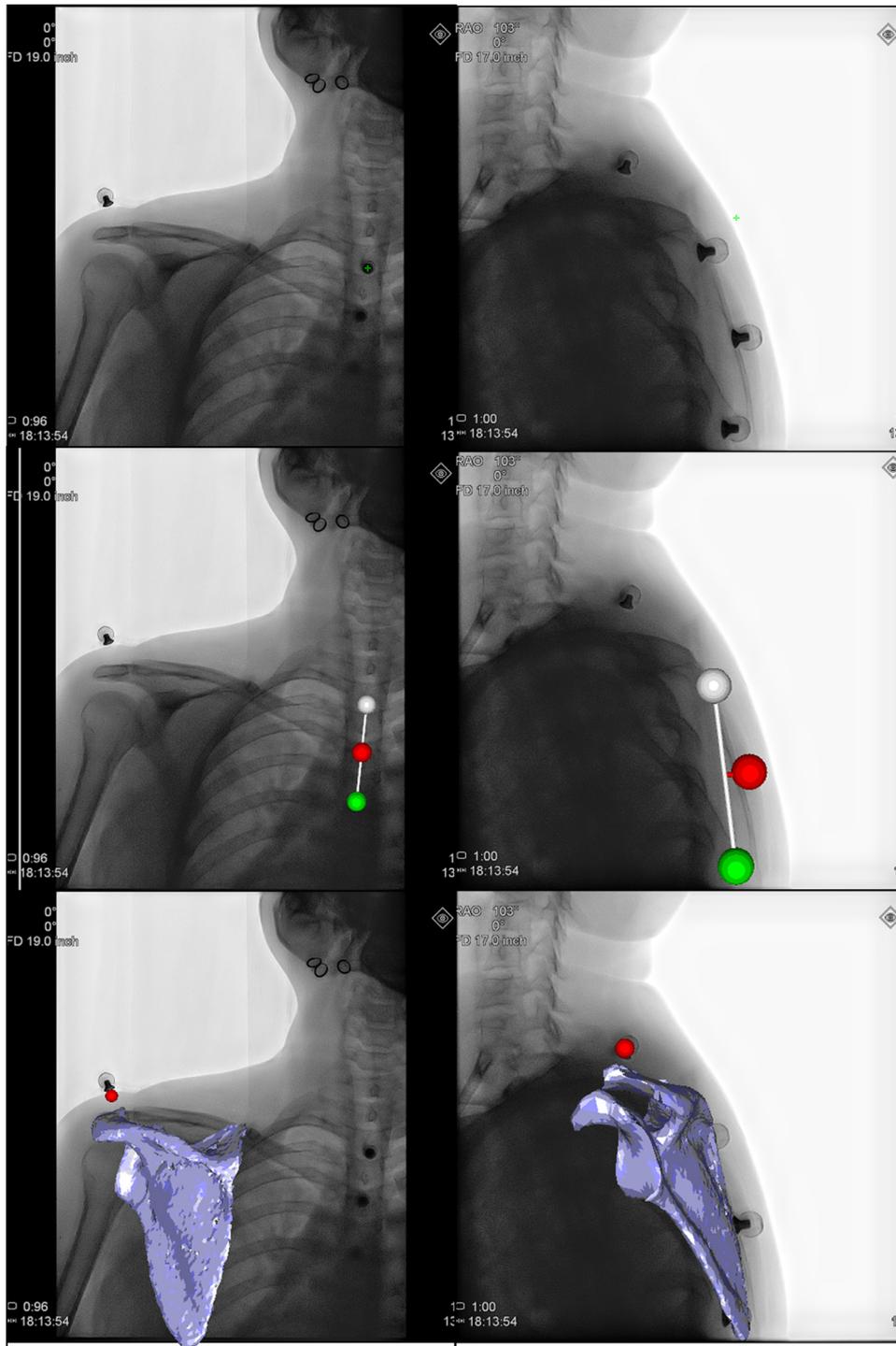
Fig. 3. The top two images show two biplane fluoroscopy images. The second row is an example of matching the 3D triad to the images to obtain trunk orientation. The third row is an example of matching the 3D scapula model to the images to obtain scapula orientation.

or the training error decreased and the test error increased. The results presented here are from the neural network configuration described above.

Table 1 shows the correlation coefficients between the neural network estimates and the fluoroscopy determined orientations. On average, the ST X correlation was very strong and the ST Z correlation was strong ($r = 0.85$ and $r = 0.78$ respectively), while the ST Y correlation was weak ($r = 0.32$). Table 2 shows the absolute mean differences between the neural network estimated ST angles and the fluoroscopy determined ST angles. While the average X, Y,

and Z absolute mean differences for all subjects were less than ten degrees, there were several subjects that exhibited absolute mean differences greater than ten degrees.

4. Discussion

Accurately measuring ST joint angles is important for understanding the kinematics and function of the shoulder and upper extremity. Current efforts to measure shoulder function often provide no information regarding the ST versus glenohumeral
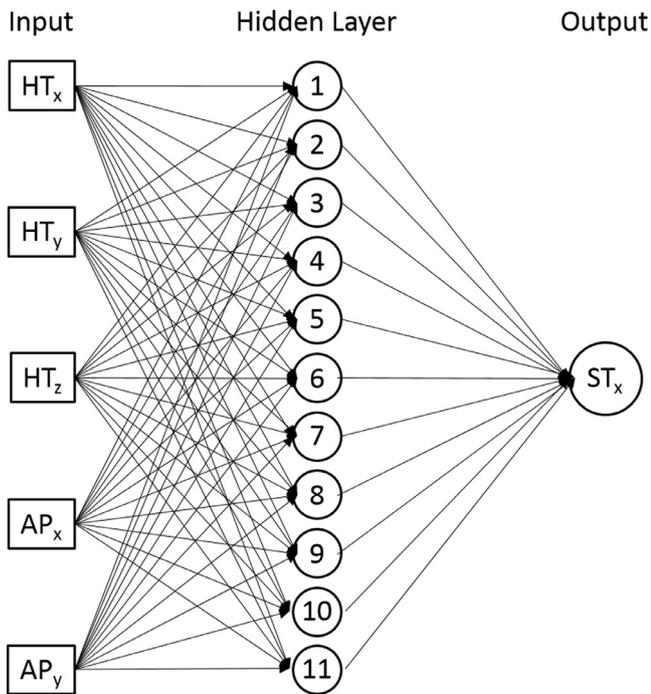
Fig. 4. The neural network configuration that performed the best had one hidden layer with eleven neurons, used a sigmoid/logistic activation function, and had a learning rate of 0.1. ST_x, ST_y, and ST_z each had their own neural network.

Table 1

Correlation coefficients between the fluoroscopy determined scapulothoracic angles and the neural network estimated scapulothoracic angles.

Fluoroscopy and neural network correlations			
Subject	ST X	ST Y	ST Z
1	0.91	0.49	0.91
2	0.89	0.64	0.59
3	0.86	−0.33	0.91
4	0.78	0.26	0.77
5	0.90	0.55	0.86
6	0.86	0.59	0.46
7	0.75	0.13	0.87
8	0.88	0.17	0.69
9	0.85	0.41	0.94
Average	**0.85**	**0.32**	**0.78**

0.00–0.19: very weak, 0.20–0.39: weak, 0.40–0.59: moderate, 0.60–0.79: strong, 0.80–1.0: very strong. ST = Scapulothoracic.

Table 2

Absolute mean differences between the fluoroscopy determined scapulothoracic angles and the neural network estimated scapulothoracic angles.

Fluoroscopy and neural network absolute mean differences (degrees)			
Subject	ST X	ST Y	ST Z
1	7.87	6.87	5.56
2	7.94	5.94	9.86
3	9.90	8.09	5.78
4	10.02[a]	10.17[a]	13.05[a]
5	7.64	6.90	6.03
6	9.35	6.54	9.35
7	10.76[a]	9.25	5.52
8	8.00	6.83	7.62
9	7.48	11.19[a]	6.81
Average	**8.78**	**7.98**	**7.73**

[a] Difference greater than 10°.
ST = Scapulothoracic.

joint contributions. Techniques that attempt to quantify these measures are often inaccurate, invasive, time consuming, induce large amounts of radiation exposure, and/or require the subject to lie horizontally in an enclosed space. Furthermore, the recommended techniques (acromion marker clusters, scapula trackers, and electromagnetic sensors) have only been validated on single plane humeral elevation and internal/external rotation. While these motions are important, there are many complex motions such as acts of daily living, throwing, upper extremity cycling, wheel chair lifts, etc. that would benefit from an accurate technique for measuring ST kinematics.

The primary goal of this study was to develop and validate a new clinically useful approach to measuring ST kinematics that would be applicable to all motions and all populations. Motion capture technology is available in many hospitals, gait laboratories, universities, and research laboratories. By using the readily available technology in an innovative way, we can develop a relationship between the humerus and scapula that can be applied to dynamic motions.

Scapulothoracic orientations estimated with the individualized neural networks were favorable. The ST upward/downward rotation (X) angles and ST anterior/posterior tilt (Z) angles estimated with machine learning algorithms correlated very strongly and strongly with the ST X and ST Z angles measured with fluoroscopy and 3D matching, respectively. The absolute mean differences, averaged for all subjects, were all below nine degrees, however, there were individuals with absolute mean differences greater than the ten degrees deemed clinically meaningful. Seventy seven percent of the ST upward/downward rotation (X) and ST internal/external rotation (Y) absolute mean differences were below ten degrees, and 89 percent of the ST anterior/posterior tilt (Z) absolute mean differences were below ten degrees.

One possible reason for the underperformance of the neural networks is that neural networks are sensitive to input values outside the range of values used to develop the networks. Although we asked subjects to strive for maximum excursion in all static positions, we found that every subject exceeded the humerothoracic X, Y, and/or Z values and the AP X and/or Y values captured in the static positions during the dynamic trials. Fig. 5 shows the values collected during the static positions, and used to develop the algorithms, versus the values captured during the dynamic trials for one subject. We see with this subject that the ballistic feature of a dynamic trial allowed the subject to reach further during motions such as abduction and extension. Anecdotally it was difficult for some subjects to maintain a position such as extension against gravity during the static collections, thus it is not surprising that they reached further during active motions. This pattern of reaching further during the dynamic trials for abduction and extension was seen in a majority of the subjects. Additionally we saw that some of the humerothoracic X, Y, and/or Z and AP X and/or Y extremes were reached while moving from one position to another, and not during the static positions themselves. For example, Fig. 3 shows that in subject 4 maximum humerothoracic extension (−Z) was reached while transitioning from hand on spine to external rotation, and maximum humerothoracic external rotation (+Y) was reached transitioning from hand to mouth to hand to neck. Additional extension was needed for the hand to clear the trunk as the subject began to externally rotate while transitioning to the external rotation position. Additional external rotation was needed for the hand to clear the head before reaching the neck.

Finding a valid and reliable method for measuring scapula motion has been a long standing challenge. There are various techniques available ranging from radiography, magnetic resonance imaging, fluoroscopy, inertial sensors, goniometers, cutaneous markers and optoelectronic systems. Cutaneous marker based solutions have been the most widely studied, as they are the
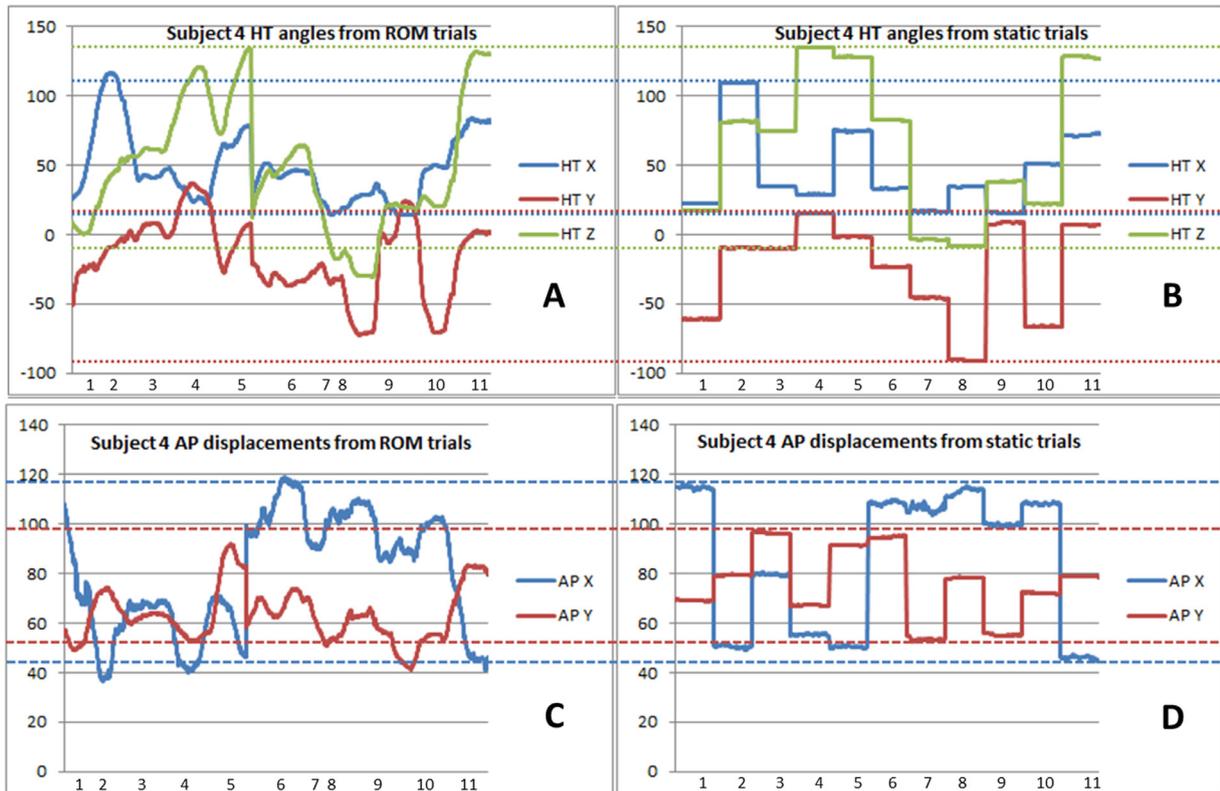
Fig. 5. Plots of the input variables (HT X, Y, Z (in degrees) and AP X, Y (in mm)) for the mathematical algorithms for Subject 4. Plots B and D show the variables used to develop the mathematical algorithms, collected during the static trials. Plots A and C show the variables used to estimate scapulothoracic orientations during the ROM trials. Horizontal lines indicate the static ranges for each variable. Every variable exceeded the static range at some point during the dynamic ROM trials. 1 = neutral, 2 = abduction, 3 = hand to mouth, 4 = hand to neck, 5 = elevation, 6 = forward reach, 7 = extension, 8 = hand on spine, 9 = external rotation, 10 = internal rotation, 11 = flexion.
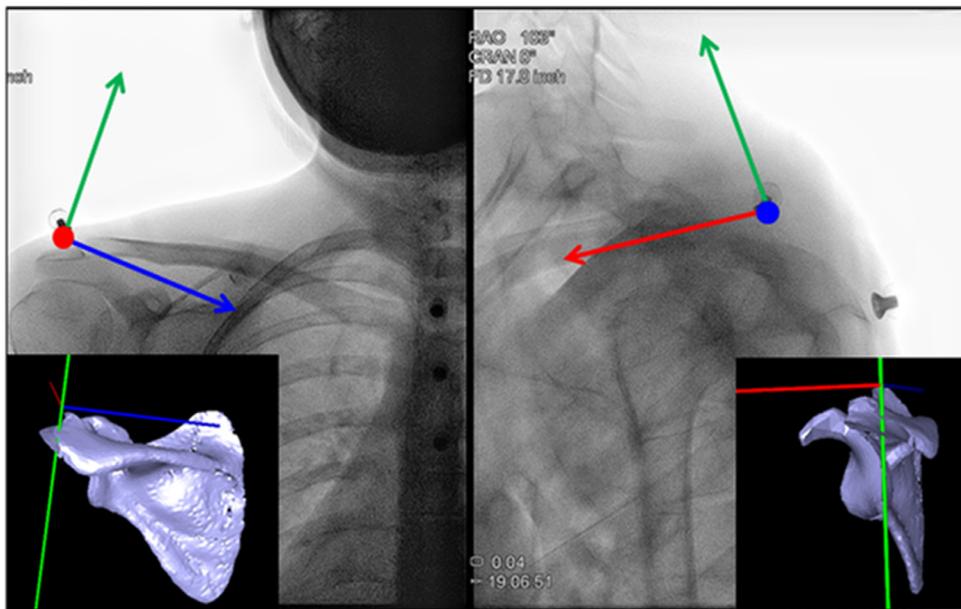

Fig. 6. Scapula coordinate systems in the biplane fluoroscope views. It is easiest to match motion about the axis perpendicular to the viewing frame. Since the Y axis (green) lies in both viewing planes, it is more difficult to match motion around the Y axis than motions about the X (red) or Z (blue) axes. (For interpretation of the references to color in this figure legend, the reader is referred to the web version of this article.)

most practical non-invasive method for implementing in a laboratory or clinical setting. In 2014 Lempereur, et al. conducted a systematic review on the validity and reliability of 3D marker based methods for measuring scapula kinematics [22]. Seventeen studies were included in the assessment of validity with errors about each axis ranging from 1.4° to 16.16° (X: 1.6° – 14.21°, Y: 1.5° −14.86°,

Z: 1.4° −16.16°). If all studies were pooled, the average X error was 5.19°, the average Y error was 5.30°, and the average Z error was 5.27°. While these average errors were slightly less than the average errors found with the neural networks ($X = 8.78°$, $Y = 7.98°$, $Z = 7.73°$), there are several key differences between this study and previous studies. Despite being a systematic review on methods

for measuring scapular kinematics, only three of the seventeen reviewed studies actually validated their measurement techniques during motion. The other fourteen studies validated their techniques with palpation or scapula locators in various static positions. The three studies that validated with scapular kinematics validated their techniques with bone pins [1,14] or biplane x-ray [23]. The average errors from these three studies are slightly higher than the average error of all studies ($X = 5.92°$, $Y = 5.57°$, $Z = 5.42°$). Another important difference is that all previous studies have examined the errors over an individual motion, the majority being only planar motions such as humeral abduction, humeral flexion, humeral elevation in the scapula plane, humeral internal rotation, and humeral external rotation. Only three studies include complex motions such as hand on spine, hand to mouth, hand to neck, and/or reach [2,14,24]. This study is the first study to look at errors over an entire shoulder range of motion, including both planar motions and complex multi-planar motions. When machine learning algorithms are developed with static positions that represent the motions of interest, the errors are well within the range of errors reported in literature, and perhaps more importantly, this technique has actually been validated with the motions of interest.

There are three main sources of error associated with this study; palpation, the matching process used as the validation reference, and the error in the algorithms themselves. Palpation introduces approximately 2 degrees of error [25], and the matching technique used for the reference validation contains approximately 7.5 degrees of error [17]. Additionally, preliminary testing of the matching technique showed that some axes are more difficult to match than others [17]. The orientation of the fluoroscopy beams allowed the scapula's X axis to be almost perpendicular to one viewing plane and the scapula's Z axis to be almost perpendicular to the other viewing plane. The scapula's Y axis, however, was parallel to both views; making movement about the scapula's Y axis particularly difficult to match (Fig. 6). Due to this difficulty, much of the error about the Y axis may have come from the matching procedure used for the validation standard and not the algorithm development.

While not perfect, the algorithms provide conceptual evidence that a clinically useful tool for measuring ST kinematics can be created from motion capture data. The use of neural networks allows for unconstrained measurement, minimizes load and pain, allows for natural, including compensatory, movements, accurately represent underlying skeletal structure and motion, work on an individual basis, and estimates scapula orientation within 10°.

Disclosures

Competing interests: None declared.

Ethical approval: The study was approved by the University of Delaware and Christiana Care Institutional Review Boards.

References

[1] Karduna AR, McClure PW, Michener La, Sennett B. Dynamic measurements of three-dimensional scapular kinematics: a validation study. J Biomech Eng 2001;123:184. doi:10.1115/1.1351892.

[2] Bourne DA, Choo AM, Regan WD, MacIntyre DL, Oxland TR. The placement of skin surface markers for non-invasive measurement of scapular kinematics affects accuracy and reliability. Ann Biomed Eng 2011;39:777–85. doi:10.1007/s10439-010-0185-1.

[3] Johnson MP, McClure PW, Karduna AR. New method to assess scapular upward rotation in subjects with shoulder pathology. J Orthop Sport Phys Ther 2001;31:81–9.

[4] Uhl TL, Ben Kibler W, Gecewich B, Tripp BL. Evaluation of clinical assessment methods for scapular dyskinesis. Arthrosc J Arthrosc Relat Surg 2009;25:1240–8. doi:10.1016/j.arthro.2009.06.007.

[5] Lin J, Hanten WP, Olson SL, Roddey TS, Soto-quijano DA, Lim HK, et al. Shoulder dysfunction assessment: self-report and impaired scapular movements. Phys Ther 2006;86:1065–74.

[6] Nishinaka N, Tsutsui H, Mihara K, Suzuki K, Makiuchi D, Kon Y, et al. Determination of in vivo glenohumeral translation using fluoroscopy and shape-matching techniques. J Shoulder Elb Surg 2008;17:319–22. doi:10.1016/j.jse.2007.05.018.

[7] Baumgarten KM, Osborn R, Schweinle WE, Eidsness J, Schelhaas D. A Novel technique for determining scapulohumeral translation: a case-control and inter-rater reliability study. Int J Sport Phys Ther 2012;7:39–48.

[8] Warner MB, Chappell PH, Stokes MJ. Measuring scapular kinematics during arm lowering using the acromion marker cluster. Hum Mov Sci 2012;31:386–96. doi:10.1016/j.humov.2011.07.004.

[9] Nicholson KF, Russo SA, Kozin SH, Zlotolow DA, Hulbert RL, Rowley KM, et al. Evaluating the acromion marker cluster as a method for measuring scapular orientation in children with brachial plexus birth palsy. J Appl Biomech 2014;30:128–33. doi:10.1123/jab.2012-0180.

[10] Xu X., Dickerson C.R., Lin J.-H., Mcgorry R.W. Evaluation of regression-based 3-D shoulder rhythms 2016. doi:10.1016/j.jbiomech.2015.07.005.

[11] Lawrence RL, Ellingson AM, Ludewig PM. Validation of single-plane fluoroscopy and 2D/3D shape-matching for quantifying shoulder complex kinematics. Med Eng Phys 2018. doi:10.1016/j.medengphy.2017.11.005.

[12] Zhang C, Skalli W, Lagacé PY, Billuart F, Ohl X, Cresson T, et al. Investigation of 3D glenohumeral displacements from 3D reconstruction using biplane X-ray images: accuracy and reproducibility of the technique and preliminary analysis in rotator cuff tear patients. J Electromyogr Kinesiol 2016. doi:10.1016/j.jelekin.2015.08.002.

[13] Richardson RT, Nicholson KF, Rapp EA, Johnston TE, Richards JG. A comparison of acromion marker cluster calibration methods for estimating scapular kinematics during upper extremity ergometry. J Biomech 2016. doi:10.1016/j.jbiomech.2016.02.052.

[14] Bourne DA, Choo AM, Regan WD, MacIntyre DL, Oxland TR. A New subject-specific skin correction factor for three-dimensional kinematic analysis of the scapula. J Biomech Eng 2009;131:121009–19.

[15] McClure PW, Michener LA, Sennett BJ, Karduna AR. Direct 3-dimensional measurement of scapular kinematics during dynamic movements in vivo. J Shoulder Elb Surg 2001;10:269–77. doi:10.1067/mse.2001.112954.

[16] Massimini DF, Warner JJP, Li G. Non-invasive determination of coupled motion of the scapula and humerus–an in vitro validation. J Biomech 2011;44:408–12. doi:10.1016/j.jbiomech.2010.10.003.

[17] Nicholson KF, Richardson RT, Miller F, Richards JG. Determining 3D scapular orientation with scapula models and biplane 2D images. Med Eng Phys 2017;41:103–8. doi:10.1016/J.MEDENGPHY.2017.01.012.

[18] Mozingo JD, Akbari Shandiz M, Marquez FM, Schueler BA, Holmes DR, McCollough CH, et al. Validation of imaging-based quantification of glenohumeral joint kinematics using an unmodified clinical biplane fluoroscopy system. J Biomech 2018. doi:10.1016/j.jbiomech.2018.02.012.

[19] Wu G, Cavanagh PR. ISB recommendations for standardization in the reporting of kinematic data. J Biomech 1995;28:1257–61.

[20] Abzug JM, Kozin SH. Current concepts: neonatal brachial plexus palsy. Orthopedics 2010;33:430–5. doi:10.3928/01477447-20100429-25.

[21] Evans JD. Straightforward statistics for the behavioral sciences. Pacific Grove, CA: Brooks/Cole Publishing; 1996.

[22] Lempereur M, Brochard S, Leboeuf F, Rémy-Néris O. Validity and reliability of 3D marker based scapular motion analysis: a systematic review. J Biomech 2014;47:2219–30. doi:10.1016/j.jbiomech.2014.04.028.

[23] Chu Y, Akins J, Lovalekar M, Tashman S, Lephart S, Sell T. Validation of a video-based motion analysis technique in 3-D dynamic scapular kinematic measurements. J Biomech 2012;45:2462–6. doi:10.1016/j.jbiomech.2012.06.025.

[24] Mattson JM, Russo SA, Rose WC, Rowley KM, Richards JG. Identification of scapular kinematics using surface mapping: a validation study. J Biomech 2012;45:2176–9. doi:10.1016/j.jbiomech.2012.05.048.

[25] de Groot JH. The variability of shoulder by means of palpation motions recorded. Clin Biomech 1997;12:461–72.